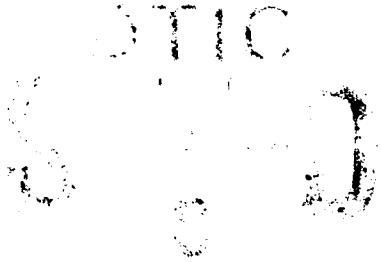

SPIRAL CRACKING AROUND A STRAINED CYLINDRICAL INCLUSION IN A BRITTLE MATERIAL AND IMPLICATIONS FOR VIAS IN INTEGRATED CIRCUITS

L. B. FREUND AND K. S. KIM
Division of Engineering, Brown University, Providence, RI 02912

ABSTRACT

The practice of forming electrical conduction paths in an insulating material by filling cylindrical holes with molten metal can result in high residual stresses when the metal cools. Residual stress is greatest near the metal-insulator interface, and stress relaxation by means of de-adhesion is possible. Another failure mode that poses greater practical difficulties is the growth of cracks along paths which spiral away from the interface into the brittle material. Such cracks may occur singly or in pairs, and their lengths can be sufficiently great to provide links with adjacent conduction paths. Such cracks are considered from the fracture mechanics point of view. The residual stress field is relaxed by the growth of spiral cracks which are modeled as continuous distributions of dislocations. It is assumed that these cracks grow so that the stress state on the prospective fracture plane just ahead of the crack tip is purely tensile. The paths are determined by means of an incremental numerical procedure.

INTRODUCTION

The question of reliability of integrated circuits is concerned with the predictable sustained performance of some electronic function. Even though the capacity for carrying mechanical loads may not be relevant to this function, failures of devices are commonly due to mechanical effects. These failures are driven by residual stresses arising from fabrication processes, often carried out at elevated temperature and involving combinations of materials with very different thermal and mechanical properties. The fracture problem studied here is of this kind.

In fabricating an integrated circuit with a complex planar or multi-planar structure, it is sometimes necessary to pass conduction lines directly through the brittle substrate of a device. This may be done by boring a hole through the thickness of the substrate, which is assumed to be initially stress free. The hole is then filled with molten metal, say aluminum or copper, and the molten metal adheres to the surface of the hole as it cools and solidifies. As a result, an elastic mismatch extensional strain $\Delta\epsilon$ can arise between the metal inclusion in the cylindrical hole and the surrounding brittle material.

If the brittle substrate is thick compared to the radius of the hole (see Figure 1), then the mechanical fields over most of the length of the inclusion are essentially two dimensional plane strain fields. This is the case studied here. The tensile stress in the residual stress field tends to be greatest at the bimaterial interface. Indeed, fractures typically nucleate at the interface. However, it is often observed that fractures grow away from the interface, and they tend to spiral around the cylindrical inclusion, as suggested in Figure 1. Furthermore, the detailed shape of the spiral appears to be quite sensitive to the relative properties of the two materials involved. The purpose here is to examine the spiral cracking process from the perspective of brittle fracture mechanics.

The stress field of a two dimensional elastic solid containing a sharp crack is nominally square root singular at the crack tips. The amplitude of this singularity is called

Presented at the 1991 MRS Spring Meeting, Anaheim, CA in Symposium H: Mechanical Behavior of Materials and Structures in Microelectronics

Fig. 1. Schematic diagram of cylindrical inclusions in a brittle material, with a spiral crack emanating from one inclusion.

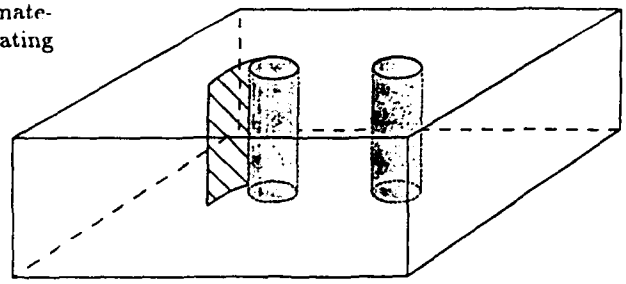

the stress intensity factor and the spatial dependence of the asymptotic field is universal. The tendency for crack growth is commonly expressed, as a postulate on material behavior, in terms of critical or material-specific values of the stress intensity factor. Of particular concern here is the connection between the *direction* of crack growth and the stress intensity factor. For plane strain deformation, the crack opening near the tip can be symmetric with respect to the local plane of the crack (mode I), antisymmetric (mode II), or some combination of the two (mixed mode). It has frequently been observed that cracks in brittle materials tend to advance in such a way as to maintain a symmetric deformation field (mode I) near the moving crack tip [1,2]. This additional postulate on fracture behavior, sometimes called the principle of local symmetry, is adopted as a criterion to predict the path of crack advance around the cylindrical inclusion.

The analysis proceeds in several steps. First, the residual stress field due to the thermal mismatch strain is estimated in the absence of a crack. Then, a crack is assumed to initiate at the interface and to grow around the inclusion. A numerical algorithm is developed for extracting the values of the mode I and mode II stress intensity factors, denoted by K_I and K_{II}, as the crack gets longer. The same procedure has been applied for straight cracks in a homogeneous body in [3]. The algorithm is sufficiently general to analyze crack growth along a path which is not specified in advance but which is selected incrementally by the local symmetry condition $K_{II} = 0$. Results are presented for cases when the stiffness of the inclusion is equal to, greater than and less than the stiffness of the surrounding brittle elastic material. Similar calculations restricted to the case of homogeneous bodies have been presented in [4] and [5].

INITIAL RESIDUAL STRESS

Suppose that a cylindrical hole of radius a exists in a stress free block of brittle material which has dimensions large compared to a. The hole is filled with molten metal which adheres to the surface of the hole as it cools. Suppose that an extensional mismatch strain $\Delta\epsilon$ results from the temperature change and/or the difference in thermal expansion coefficients. The axially symmetric stress distribution in the surrounding material, referred to polar coordinates centered on the hole, is

$$\sigma^0_{rr} = -\sigma^0_{\theta\theta} = \frac{2\mu\mu_m(1+\nu_m)^2\Delta\epsilon}{\mu_m(1+\nu_m)+\mu(1-\nu_m)}\frac{a^2}{r^2} \equiv \frac{\mu C}{2\pi(1-\nu)}\frac{a^2}{r^2}, \quad \sigma^0_{r\theta} = 0 \qquad (1)$$

where μ and ν are the shear modulus and Poisson's ratio, respectively, of the brittle insulator and μ_m and ν_m are the corresponding constants for the inclusion. The stress (1) is to be relieved through the process of spiral cracking. All computed results for stress

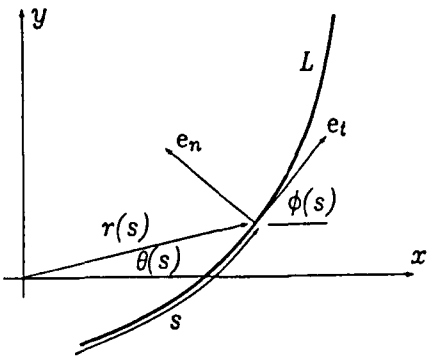

Fig. 2. A curve $\mathcal{L}$ with arclength parameter s in the range $s_- < s < s_+$, representing a possible fracture path in the x, y-plane.

are scaled by the dimensionless constant

$$C = \frac{4\pi\mu_m(1-\nu)(1+\nu_m)^2}{\mu_m(1+\nu_m)+\mu(1-\nu_m)}\Delta\epsilon \tag{2}$$

introduced in (1). When the elastic properties of the inclusion and the surrounding brittle material are approximately equal then C has a value about ten times the elastic mismatch strain $\Delta\epsilon$. All values of stress intensity factor calculated here are normalized by

$$K^* = \frac{\mu C\sqrt{a}}{2(1-\nu)} \tag{3}$$

To give an indication of the value of this normalizing parameter for a particular system, consider an inclusion with radius $a \sim 0.1\,mm$ and mismatch strain of 0.001 in a material with shear modulus of about $30\,GPa$. These numerical values imply that $K^* \sim 2\,MPa\sqrt{m}$.

THE SUPERPOSITION SCHEME

Consider any curve in the plane that is a prospective path for a spiral crack, and denote this curve by $\mathcal{L}$. A pair of orthogonal unit vectors $\mathbf{e}_t$, $\mathbf{e}_n$ aligned with the tangent and normal to $\mathcal{L}$ are introduced, as shown in Figure 2. The variable s is the arclength along $\mathcal{L}$ measured in the direction of $\mathbf{e}_t$ from some arbitrary point. The angle $\phi(s)$ is the angle measured counterclockwise from the x-axis to the tangent line of $\mathcal{L}$ at s. For any state of stress in the body expressed with respect to the polar coordinate directions or the underlying x, y rectangular coordinate directions, the normal traction $\tau_n(s)$ and the shear traction $\tau_t(s)$ associated with the normal vector $\mathbf{e}_n$ at any point along $\mathcal{L}$ can be expressed as the complex quantity

$$\begin{aligned}\tau_n(s) + i\tau_t(s) &= \tfrac{1}{2}(\sigma_{xx}+\sigma_{yy}) + \left[\tfrac{1}{2}(\sigma_{yy}-\sigma_{xx}) + i\sigma_{xy}\right] e^{2i\phi(s)} \\ &= \tfrac{1}{2}(\sigma_{rr}+\sigma_{\theta\theta}) + \left[\tfrac{1}{2}(\sigma_{\theta\theta}-\sigma_{rr}) + i\sigma_{r\theta}\right] e^{2i[\phi(s)-\theta(s)]}\end{aligned} \tag{4}$$

where $i = \sqrt{-1}$. In this expression, it is understood that the coordinate s on $\mathcal{L}$, coordinates x, y in the plane, and coordinates r, θ in the plane represent the same point.

In terms of the representation (4) and the residual stress (1), the traction to be relieved by crack growth is $\sigma_n^0(s) + i\sigma_t^0(s)$. The process of crack growth is simulated by introducing a continuously distributed array of Volterra elastic dislocations for which the

distribution is selected to cancel the initial residual stress. This is a common device for analyzing fracture phenomena in brittle materials [6]. The fundamental building block in the procedure is the expression for the complete stress field due to a single, isolated dislocation with arbitrary Burgers vector at an arbitrary point in the elastic body being analyzed. In the present case, the body is the whole plane with elastic constants E and ν containing an embedded circular inclusion of radius a with elastic constants E_m and ν_m.

This stress distribution can be found without approximation as outlined in Appendix I. Features of particular significance for this development are that each stress component is linear in the components of the Burgers vector of the dislocation and that each stress distribution has a pole-type singularity at the point coinciding with the dislocation in the plane. Consider once again the arbitrary curve $\mathcal{L}$. Suppose the dislocation is located at a point on that curve identified by a particular value of arclength, say s, and that the Burgers vector of that dislocation is denoted by components $b_x(s)$ and $b_y(s)$. Now consider any other point on $\mathcal{L}$ located by means of a value of arclength q. The features of the stress distribution noted above imply that the traction components σ_n and σ_t at q due to the dislocation at s can be written in the form

$$\begin{aligned}\sigma_n(q;s) &= \frac{1}{s-q}\left[\Sigma_{nx}(q,s)b_x(s) + \Sigma_{ny}(q,s)b_y(s)\right] \\ \sigma_t(q;s) &= \frac{1}{s-q}\left[\Sigma_{tx}(q,s)b_x(s) + \Sigma_{ty}(q,s)b_y(s)\right]\end{aligned} \tag{5}$$

The steps required to evaluate the four functions $\Sigma_{nx}(q,s),\ldots$ appearing in (5) for any values of s and q are given in detail in Appendix II. These functions play a central role in the solution procedure.

The stress fields discussed above are now generalized from the case of a single, isolated dislocation with finite Burgers vector to the case of a continuous distribution of dislocation with infinitesimal Burgers vectors. This transition is effected simply by making the replacements

$$b_x(s) \to \psi_x(s)ds \text{ and } b_y(s) \to \psi_y(s)ds \tag{6}$$

and then allowing the arclength s to range over values $s_- < s < s_+$ on $\mathcal{L}$. With this interpretation, $\psi_i(s)ds$ represents the net Burgers displacement in the i-direction of a dislocation smeared out over the infinitesimal interval from s to $s+ds$. In other words, $\psi_i(s)$ is the gradient along $\mathcal{L}$ of the discontinuity in the i-component of displacement across $\mathcal{L}$ at s. If the discontinuity in displacement u_i at s is denoted by $[\![u_i]\!](s)$, then

$$[\![u_x]\!](q) = \int_{s_-}^{q} \psi_x(s)\,ds\,, \quad [\![u_y]\!](q) = \int_{s_-}^{q} \psi_y(s)\,ds \tag{7}$$

where it is tacitly assumed that the crack is closed without net dislocation at $s = s_-$. If the same is true at $s = s_+$ then ψ_x and ψ_y are subject to the closure conditions

$$\int_{s_-}^{s_+} \psi_x(s)\,ds = 0\,, \quad \int_{s_-}^{s_+} \psi_y(s)\,ds = 0 \tag{8}$$

The functions ψ_x and ψ_y are expected to be square-root singular at the crack ends [6] and to be asymptotically proportional to the elastic stress intensity factors there. In terms of the mode I and mode II stress intensity factors discussed in the Introduction, this asymptotic relationship is

$$K_{II} + iK_I = -\frac{\mu}{2(1-\nu)} \lim_{s\to s_+} \sqrt{2\pi(s_+ - s)}\left[\psi_x(s) + i\psi_y(s)\right]e^{-i\phi(s)} \tag{9}$$

For the continuously distributed dislocations, the traction at any point q on $\mathcal{L}$ is still given by (5), provided that the expressions on the right side of (5) are summed over all values of s. This is accomplished by making the replacements (6) in (5), and then integrating over the full range of s on $\mathcal{L}$. The result is

$$\begin{aligned}\sigma_n(q) &= \int_{s_-}^{s_+} \left[\Sigma_{nx}(q,s)\psi_x(s) + \Sigma_{ny}(q,s)\psi_y(s)\right]\frac{ds}{s-q} \\ \sigma_t(q) &= \int_{s_-}^{s_+} \left[\Sigma_{tx}(q,s)\psi_x(s) + \Sigma_{ty}(q,s)\psi_y(s)\right]\frac{ds}{s-q}\end{aligned} \tag{10}$$

Thus, if the curve representing the crack line $\mathcal{L}$ is known, and the distribution of crack opening $\psi_x(s), \psi_y(s)$ along the curve is known, then (10) provides the means of calculating the distribution of *traction* on the crack faces that is required to enforce the given opening.

The problem at hand, however, is the inverse of this situation. That is, the traction is given along any possible fracture path by the distribution of initial residual stress in the brittle region (1). The distribution of relative displacement of the crack faces along the crack path is unknown and, indeed, the path $\mathcal{L}$ itself is unknown a priori. Thus, a strategy is required for determining the crack path and the distribution of crack opening required to relax the initial residual stress in a physically realistic way. The growth of the crack negates the traction induced by the initial residual stress field on the crack path. This implies that the crack opening is sought for which

$$\sigma_n(q) + \sigma_n^0(q) = 0 \text{ and } \sigma_t(q) + \sigma_t^0(q) = 0 \text{ along } \mathcal{L} \tag{11}$$

In view of (10), these conditions yield singular integral equations for the crack opening distribution $\psi_x(s)$ and $\psi_y(s)$.

A common crack growth criterion for brittle materials of the kind imagined here is that the crack advances with $K_I = K_{Ic}$ and $K_{II} = 0$ where K_{Ic} is the constant fracture toughness of the material. Indeed, the spiral shape of observed fracture paths in consistent with this hypothesis, and qualitative observations suggest that the condition $K_{II} = 0$ may be the precise mechanism by which the cracks search out the spiral paths which they follow. This idea is pursued in the next section by letting the crack seek a path incrementally during growth according to this criterion.

CRACK PATHS BASED ON $K_{II} = 0$

The crack is assumed to start at the point $x = a$, $y = 0$ and to grow in the direction of increasing angle θ. The shape of the path is described by means of values of the slope of the path $\phi(s)$ at discrete points. If the arclength along the path is measured from the nucleation point, then the discrete points are identified by the values $s = s_k$, $k = 1, 2, 3, \ldots$ and the values of the slope at these points are denoted by $\phi(s_k) = \phi_k$. It is assumed that the path segments between those points are circular arcs, and that the slope of the path is continuous at each junction of adjacent circular arcs. The slope of the path between s_k and s_{k+1} is linear is s and is given by

$$\phi(s) = \phi_k \frac{s_{k+1} - s}{s_{k+1} \quad s_k} + \phi_{k+1} \frac{s - s_k}{s_{k+1} \quad s_k}, \quad s_k < s < s_{k+1} \tag{12}$$

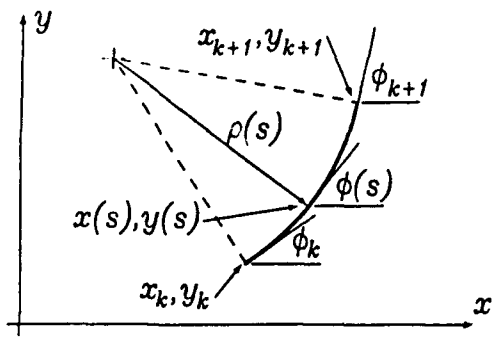

Fig. 3. An increment of the unknown crack path for $s_k < s < s_{k+1}$ represented as a circular arc with known endpoints.

The radius of curvature $\rho(s)$ of the path, constant within each segment, is

$$\frac{1}{\rho(s)} = \phi'(s) = \frac{\phi_{k+1} - \phi_k}{s_{k+1} - s_k}, \quad s_k < s < s_{k+1} \tag{13}$$

If the rectangular coordinates of the point located by s_k are (x_k, y_k), then it is evident from Figure 3 that the coordinates of any point in the interval $s_k < s < s_{k+1}$ are

$$x(s) = x_k + \rho(s)\,[\sin\phi(s) - \sin\phi_k]\,, \quad y(s) = y_k - \rho(s)\,[\cos\phi(s) - \cos\phi_k] \tag{14}$$

The quantities $r(s)$ and $\theta(s)$ needed for the calculation are readily obtained from these rectangular coordinates. A similar description has been used in [4].

With $r(s)$, $\theta(s)$ and $\phi(s)$ determined explicitly, the functions $\Sigma_{ij}(q,s)$ appearing in (10) can be evaluated by following the steps outlined in Appendix II. These functions are bounded and continuous for the class of curves $\mathcal{L}$ being considered here. With the left side of the equation (10) given in terms of the initial residual stress distribution according to (1), the equations provide a pair of coupled singular integral equations of the first kind for $\psi_x(s)$ and $\psi_y(s)$. Accurate approximate solutions to equations of this type can be found by Gaussian integration procedures [7]. To this end, the unknown functions are expressed in the form

$$\psi_x(s) = \frac{g_x(s)}{\sqrt{(s_+ - s)(s - s_-)}}, \quad \psi_y(s) = \frac{g_y(s)}{\sqrt{(s_+ - s)(s - s_-)}} \tag{15}$$

to reflect the anticipated square root singularities in these functions at the ends of the crack. The functions $g_x(s)$ and $g_y(s)$ are expected to be bounded and continuous, and to be expressible to any degree of accuracy as a finite series of Chebyshev polynomials of the first kind. The weight function appearing in the orthogonality relationship for these polynomials is

$$w(s) = \frac{1}{\sqrt{(s_+ - s)(s - s_-)}} \tag{16}$$

which is provided by the representation (15). The smooth functions $g_x(s)$ and $g_y(s)$ are represented by a series of the first N Chebyshev polynomials with unknown coefficients. The equations (10) are then enforced at the $N-1$ discrete points

$$\eta_k = \tfrac{1}{2}(s_+ + s_-) + \tfrac{1}{2}(s_+ - s_-)\cos\frac{\pi k}{N}, \quad k = 1, \ldots, N-1 \tag{17}$$

and the integrals are approximated by the appropriate Gaussian integration formulas [8], providing $2N-2$ equations for the $2N$ unknown values $g_x(s_i)$ and $g_y(s_i)$ for $i = 1, \ldots, N$.

The Gaussian integration points are

$$s_i = \tfrac{1}{2}(s_+ + s_-) + \tfrac{1}{2}(s_+ - s_-)\cos\frac{\pi(2i-1)}{N}, \quad i = 1, \ldots, N \tag{18}$$

and the full system of $2N - 2$ equations is

$$\begin{aligned} \frac{\pi}{N}\sum_{i=1}^{N}\left[\frac{\Sigma_{nx}(q_k, s_i)g_x(s_i) + \Sigma_{ny}(q_k, s_i)g_y(s_i)}{s_i - q_k}\right] &= -\sigma_n^0(q_k) \\ \frac{\pi}{N}\sum_{i=1}^{N}\left[\frac{\Sigma_{tx}(q_k, s_i)g_x(s_i) + \Sigma_{ty}(q_k, s_i)g_y(s_i)}{s_i - q_k}\right] &= -\sigma_t^0(q_k) \end{aligned} \tag{19}$$

The remaining two equations are obtained from the conditions (8) that the crack closes with zero net dislocation over its entire length. Approximation of (8) by means of the Gaussian integration formula yields

$$\sum_{i=1}^{N} g_x(s_i) = 0, \quad \sum_{i=1}^{N} g_y(s_i) = 0 \tag{20}$$

Although the coefficients of the system of equations are algebraically complicated, they are known explicitly and the equations are readily solved numerically by means of the Gauss-Jordan method or an equivalent method.

Suppose that the path has been found for $0 < s < s_k$. Then the process of locating point s_{k+1} by enforcing the condition $K_{II} = 0$ is as follows. First, the length of the increment $ds \equiv s_{k+1} - s_k$ is specified. Then, the mode II stress intensity factor is calculated for three trial selections of ϕ_{k+1}, namely, $\phi_{k+1}^- = \phi_k - \epsilon$, $\phi_{k+1}^0 = \phi_k$ and $\phi_{k+1}^+ = \phi_k + \epsilon$ where ϵ is a specified small number, typically about 0.02. The three corresponding values of mode II stress intensity factor, say K_{II}^-, K_{II}^0 and K_{II}^+, then permit a parabolic interpolation for K_{II} versus ϕ_{k+1}. The root for $K_{II} = 0$ provides a first approximation for the desired value of ϕ_{k+1}. The value of K_{II} corresponding to this root is then calculated. If the value is less in magnitude than some predetermined magnitude, typically $0.001\,K_I$, then the process is terminated. If this condition is not fulfilled, then the root is used as the basis for a second iteration following the template outlined above. The process is repeated until convergence is achieved, whereupon the step to locate s_{k+2} is begun.

Representative results for the variation of mode I stress intensity factor with arclength along the computed crack paths are shown in Figure 4 for the case when $\mu_m = \mu$ and $\nu_m = \nu$, in Figure 5 when $\mu_m = 2\mu$ and $\nu_m = \nu$, and in Figure 6 when $\mu_m = \mu/2$ and $\nu_m = \nu$. The corresponding crack paths are also shown as insets in the figures. Some qualitative features are evident from the calculated shapes of the spiral cracks. For example, an increase in the stiffness ratio μ_m/μ causes the crack to spiral away from the inclusion at a faster rate.

CONCLUDING REMARKS

There are no exact elasticity solutions for spiral cracks in bi-materials systems of the type considered here. Consequently, the accuracy of the numerical algorithm for solving problems could be ascertained only by considering some limiting cases. When the two materials have the same elastic properties, that is when $\alpha = \beta = 0$, there are

Fig. 4. Mode I stress intensity factor versus crack length for the case when the two materials have identical elastic properties. The inset shows the computed crack path.

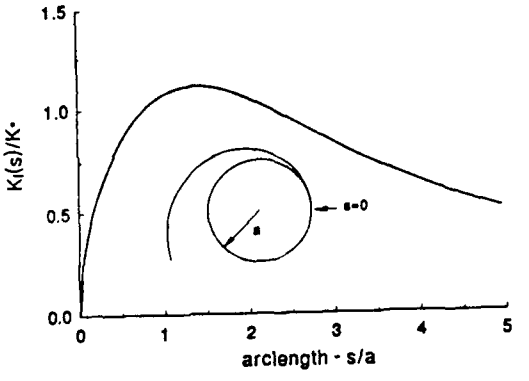

Fig. 5. Mode I stress intensity factor versus crack length for $\mu_m = 2\mu$, and the computed crack path.

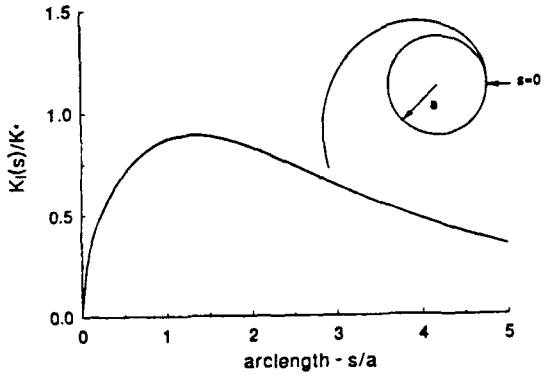

Fig. 6. Mode I stress intensity factor versus crack length for $\mu_m = \mu/2$, and the computed crack path.

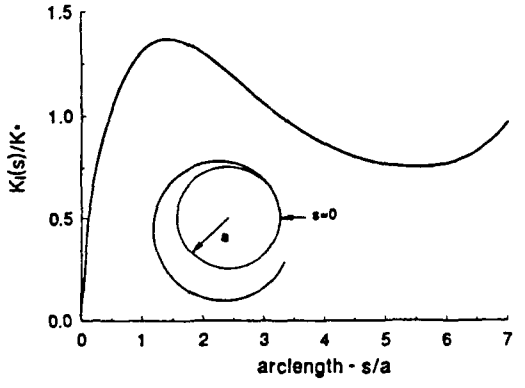

several solutions available for cracks that are straight or are circular arcs concentric with the interface. In such cases, the computed stress intensity factors agreed with the exact results to within 0.1% for $N = 15$. There is also an elastic crack solution for the case of distinct material properties but with the crack lying in the circular interface and extending over an arbitrary arc of the interface [9,10]. However, the present analysis is not applicable to the case of an interface crack, and this matter is currently being pursued.

The feature that each curve for mode I stress intensity factor has a local maximum at a value of s/a of about unity is interpreted in the following way. If a crack is nucleated at some point on the interface between the cylinder and the surrounding matrix and it

subsequently grows along a spiral path with more or less constant fracture toughness, then that growth is initially unstable. For any crack length between zero and the length when K_I is maximum, the crack grows into a region of increasing stress intensity factor. Thus, growth is spontaneous in this region. Beyond the maximum point the growth is stabilized. The actual process is probably more complex than this simple idea suggests, perhaps involving some dynamic crack growth phase.

A point of some practical significance is that the spiral cracks continue to grow away from the inclusion if the inclusion is significantly stiffer than the surrounding insulator. On the other hand, if the inclusion is significantly less stiff than the insulator, then the radial range of the spiral crack appears to be limited. Consequently, a reduction of stiffness of the inclusion by material selection or leaving a hollow core would tend to diminish the prospect of inclusion-to-inclusion cracking.

ACKNOWLEDGEMENT

This work was supported by the Office of Naval Research through Contracts N00014-90-J-4051 and N00014-90-J-1295 with Brown University. KSK acknowledges valuable discussion with Dr. R. Lacomb of IBM Corp.

REFERENCES

1. F. Erdogan and G. C. Sih, *J. Basic Engrg.* **85D**, 519 (1963).
2. R. V. Goldstein and R. L. Salganik, *Int. J. Frac.* **10**, 506 (1974).
3. M. D. Thouless, A. G. Evans, M. F. Ashby and J. W. Hutchinson, *Acta. Metall.* **35**, 1333 (1987).
4. N. A. Fleck, *Proc. R. Soc. Lond.* **A432**, 55 (1991).
5. H. Horii and S. Nemat-Nasser, in *Advances in Aerospace Structures and Materials*, edited by R. M. Laurenson and U. Yuceoglu (ASME, New York, 1982), p. 75.
6. R. W. Lardner, *Mathematical Theory of Dislocations and Fracture*, (University of Toronto Press, Toronto, 1974), p. 150.
7. L. M. Delves and J. L. Mohamed, *Computational Methods for Integral Equations*, (Cambridge University Press, 1985), p. 287.
8. P. J. Davis and I. Polonsky, in *Handbook of Mathematical Functions*, edited by M. Abramowitz and I. A. Stegun (Dover, New York, 1965), p. 887.
9. M. Toya, *J. Mech. Phys. Solids* **22**, 325 (1974).
10. A. B. Perlman and G. C. Sih, Int. J. Engrg. Sci. **5**, 845 (1967).
11. J. Dundurs and T. Mura, *J. Mech. Phys. Solids* **12**, 177 (1964).

APPENDIX I: STRESS FIELD DUE TO A SINGLE DISLOCATION NEAR A CIRCULAR INCLUSION

The configuration for which the fundamental dislocation solution is required is shown in Figure 7. The dislocation is located at a point with polar coordinates r_d, θ_d. The Burgers vector of the dislocation has rectangular components b_x and b_y. The mechanical field of the dislocation is conveniently described in rectangular coordinates oriented so that the dislocation lies on one coordinate axis. Thus, the rotated (ξ, η) rectangular coordinate system is introduced as shown in the figure. For any given point (x, y) in the

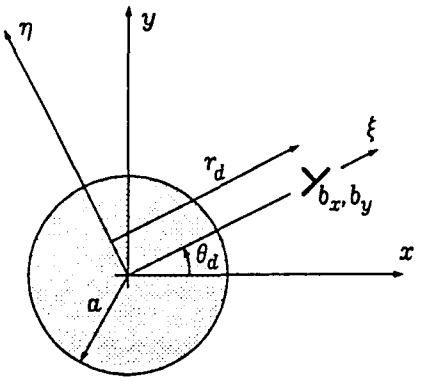

Fig. 7. Configuration which provides the fundamental elastic dislocation solution necessary to formulate integral equations modeling spiral crack growth.

original coordinate system and any Burgers vector (b_x, b_y), the corresponding position in the rotated coordinates is

$$\xi = x\cos\theta_d + y\sin\theta_d\,, \quad \eta = -x\sin\theta_d + y\cos\theta_d \tag{21}$$

and the corresponding Burgers vector is

$$b_\xi = b_x\cos\theta_d + b_y\sin\theta_d\,, \quad b_\eta = -b_x\sin\theta_d + b_y\cos\theta_d \tag{22}$$

In the rotated coordinate system, the Airy stress function for the stress distribution outside the inclusion has been given by Dundurs and Mura [11] as

$$\begin{aligned}
\chi(\xi,\eta) = &-\frac{\mu b_\xi}{2\pi(1-\nu)}\left\{\eta\ln r_1 + \frac{\alpha+\beta^2}{1-\beta^2}\eta\ln\frac{r_2}{r} + \frac{\beta(1+\alpha)}{1-\beta^2}(\xi - a^2/r_d)(\omega_2-\omega)\right.\\
&\left.-\frac{\eta(\alpha-\beta)}{2(1+\beta)}\left[\frac{(a/r_d)^4(r_d^2/a^2-1)(2\xi r_d - a^2 - r_d^2)}{r_2^2} + \frac{a^2}{r^2}\right]\right\}\\
&+\frac{\mu b_\eta}{2\pi(1-\nu)}\left\{(\xi - r_d)\ln r_1 + \frac{\alpha+\beta^2}{1-\beta^2}\left[(\xi - a^2/r_d)\ln r_2 - \xi\ln r\right] - \frac{\beta(1+\alpha)}{1-\beta^2}\eta(\omega_2-\omega)\right.\\
&-\frac{\alpha-\beta}{2(1+\beta)}\left[(a/r_d)^4(r_d^2/a^2-1)\left(2\frac{a^2}{r_d^2}\ln r_2 - \frac{(\xi-a^2/r_d)(\xi-r_d)}{r_2^2} + \frac{\eta^2}{r_2^2}\right) + \frac{a^2\xi}{r^2}\right]\\
&\left.+\left[\frac{2(\alpha-\beta)}{1+\beta}(r_d^2/a^2-1) + \frac{1+\alpha}{1-\beta} - \frac{1-\alpha^2}{(1-\beta)(1+\alpha-2\beta)}\right]\frac{a^2}{2r_d}\ln r\right\}
\end{aligned} \tag{23}$$

where

$$\begin{aligned}
r &= \sqrt{\xi^2+\eta^2}\,, \quad r_1 = \sqrt{(\xi-r_d)^2+\eta^2}\,, \quad r_2 = \sqrt{(\xi - a^2/r_d)^2+\eta^2}\\
\omega &= \arctan[\eta/\xi]\,, \quad \omega_1 = \arctan[\eta/(\xi-r_d)]\,, \quad \omega_2 = \arctan[\eta/(\xi-a^2/r_d)]
\end{aligned} \tag{24}$$

and the material parameters α and β are defined by

$$\alpha = \frac{\mu_m(1-\nu) - \mu(1-\nu_m)}{\mu_m(1\quad\nu) + \mu(1\quad\nu_m)}\,, \quad \beta = \frac{\mu_m(1-2\nu) - \mu(1-2\nu_m)}{2[\mu_m(1\quad\nu) + \mu(1\quad\nu_m)]} \tag{25}$$

For the special case when the two materials are the same, $\alpha = \beta = 0$ and the stress function for the region exterior to the inclusion is

$$\chi(\xi,\eta) = \frac{\mu}{4\pi(1-\nu)}\left[b_\eta(\xi - r_d) - b_\xi\eta\right]\ln\left(\eta^2 + (\xi - r_d)^2\right) \tag{26}$$

In either case, the stress components referred to the rectangular ξ,η-coordinate system are derived from the Airy stress function according to

$$\sigma_{\xi\xi} = \frac{\partial^2\chi}{\partial\eta^2} \qquad \sigma_{\eta\eta} = \frac{\partial^2\chi}{\partial\xi^2} \qquad \sigma_{\xi\eta} = -\frac{\partial^2\chi}{\partial\xi\partial\eta} \tag{27}$$

Finally, the stress components in the original rectangular x,y-coordinate system are obtained by the fundamental transformation rule for the stress tensor, given in complex notation by

$$\tfrac{1}{2}(\sigma_{yy} + \sigma_{xx}) = \tfrac{1}{2}(\sigma_{\xi\xi} + \sigma_{\eta\eta}), \quad \tfrac{1}{2}(\sigma_{yy} - \sigma_{xx}) + i\sigma_{xy} = \left[\tfrac{1}{2}(\sigma_{\eta\eta} - \sigma_{\xi\xi}) + i\sigma_{\xi\eta}\right]e^{-2i\theta_d} \tag{28}$$

The mathematical expressions for stress components as functions of x and y can be obtained explicitly for general values of the elastic constants. However, the expressions are too complex to be either interesting or useful. Nonetheless, the steps outlined here for constructing these expressions can be implemented in a numerical procedure in order to calculate values of these stress components without approximation.

APPENDIX II: STEPS IN CALCULATING $\Sigma_{nx}(q,s)$

Consider a crack path $\mathcal{L}$ in the plane exterior to the circular inclusion. The path is specified parametrically by polar coordinates $r(q), \theta(q)$ of each point in terms of arclength q along $\mathcal{L}$ at the point. If a dislocation is located at a particular point defined by arclength $q = s$ on $\mathcal{L}$, then the distribution of traction as a function of position q along $\mathcal{L}$ is singular as $(q-s)^{-1}$. The function $\Sigma_{nx}(q,s)$ is the amplitude of this singularity for the *normal* traction due to the x-component of the Burgers vector of the displacement. The purpose of this section is to state the steps involved in actually calculating this amplitude from the dislocation solution in the previous section.

If the position of the dislocation is specified by a particular value of arclength s then the parameters r_d and θ_d of Appendix I are replaced by $r(s)$ and $\theta(s)$, respectively.

(i) The first step in the process is to calculate the stress components $\sigma_{\xi\xi}(\xi,\eta)\ldots$ for arbitrary Burgers vector b_ξ, b_η. This requires that the the stress function (23) must be differentiated according to (27), a task most easily accomplished by means of a computer program capable of symbolic mathematical operations.

(ii) To find the particular component of interest here, set $b_x = 1$ and $b_y = 0$. Then make the substitutions implied by (22) in the expressions for stress, that is, substitute $b_\xi \to \cos\theta(s)$ and $b_\eta \to -\sin\theta(s)$ into $\sigma_{\xi\xi}(\xi,\eta)$ and the other stress components.

(iii) Next, it is necessary to transform coordinates from the ξ,η system to the fixed coordinates x,y in the physical plane. For a particular field point on $\mathcal{L}$ represented by arclength q along the curve, $x = r(q)\cos\theta(q)$ and $y = r(q)\sin\theta(q)$. Thus, the coordinate transformation indicated by (21) takes the form

$$\xi \to r(q)\cos[\theta(q) - \theta(s)], \quad \eta \to r(q)\sin[\theta(q) - \theta(s)] \tag{29}$$

(iv) At this point, the stress components are expressed in terms of the coordinates s and q along $\mathcal{L}$, and the only task remaining is to transform these stress components

to the local t, n coordinate system on $\mathcal{L}$ according to (4). For the particular stress component of interest, this is accomplished by

$$\begin{aligned}\Sigma_{nt}(q,s) &= \tfrac{1}{2}[\sigma_{\xi\xi}(q,s) + \sigma_{\eta\eta}(q,s)] \\ &+ \tfrac{1}{2}[\sigma_{\eta\eta}(q,s) - \sigma_{\xi\xi}(q,s)]\cos 2[(\phi(q) - \theta(s)] - \sigma_{\xi\eta}(q,s)\sin 2[\phi(q) - \theta(s)]\end{aligned} \tag{30}$$

These steps are readily implemented in a computational procedure. It is noted that the implementation requires no approximation in the calculation of the factors $\Sigma_{ij}(q,s)$ for any values of q and s.